C. R. Chimie 5 (2002) 713–724

S1631074802014406/REV

Nanoscale phase separation effects near $\bar{r} = 2.4$ and 2.67, and rigidity transitions in chalcogenide glasses

Punit Boolchand*, Daniel G. Georgiev, Tao Qu, Fei Wang, Liuchun Cai, Swapnajit Chakravarty

Department of Electrical, Computer Engineering and Computer Science, University of Cincinnati, Cincinnati, Ohio 452221-0030, USA

Received 24 April 2002; accepted 2 July 2002

Abstract – Nanoscale phase separation effects are of general interest in glass science. Such structural effects produce usually pronounced changes in glass physical properties which can mask the more subtle elastic effects related to rigidity transitions. The glass-transition temperature, T_g, is an intrinsic measure of network connectivity. It can be expected to increase or decrease as a network polymerizes or nanoscale phase separates. Compositional trends in $T_g(x)$ in binary As_xSe_{1-x} and Ge_ySe_{1-y} glasses show thresholds near the stoichiometric compositions, $x = 2/5$ or a mean coordination number $\bar{r} = 2.4$, $y = 1/3$ or $\bar{r} = 2.67$. These T_g trends in conjunction with spectroscopic (Raman, Mössbauer) evidence of broken chemical order suggest that the stoichiometric glasses As_2Se_3 and $GeSe_2$ consist of a Se-rich majority phase that is separate from a compensating Ge- or As-rich minority phase, i.e., they are *nanoscale phase separated*. On the other hand, ternary $Ge_x(As \text{ or } P)_xSe_{1-2x}$ glasses containing equal proportions of the group IV and V elements reveal compositional trends in $T_g(x)$ that increase monotonically with x; they appear to polymerize increasingly over a wide $2 < r < 2.8$ range of connectivities and are homogeneous. In these ternary glasses, *experimental evidence for rigidity transitions is observed near* $\bar{r} = 2.40$. Previous claims of a rigidity transition near $\bar{r} = 2.67$ can be traced to nanoscale phase separation effects. ***To cite this article: P. Boolchand et al., C. R. Chimie 5 (2002) 713–724***

nanoscale phase separation effects / rigidity transitions / chalcogenide glasses / Raman / Mössbauer

Résumé – Les effets de séparation de phase à l'échelle nanométrique sont d'intérêt général en science du verre. De tels effets structuraux produisent d'ordinaire des changements prononcés des propriétés physiques du verre, qui peuvent masquer les effets élastiques plus subtils liés aux transitions de rigidité. La température de transition vitreuse, T_g, constitue une mesure intrinsèque de la connectivité du réseau. On peut s'attendre à un accroissement ou à une diminution lorsqu'un réseau polymérise ou qu'une phase d'échelle nanométrique se sépare. Les tendances compositionnelles de $T_g(x)$ dans les verres binaires As_xSe_{1-x} et Ge_ySe_{1-y} font apparaître des seuils près des compositions stœchiométriques, $x = 2/5$, ou un nombre moyen de coordination $\bar{r} = 2.4$, $y = 1/3$ ou $\bar{r} = 2.67$. Ces tendances de T_g, conjointement avec la preuve spectroscopique (Raman, Mössbauer) d'un ordre chimique brisé, suggèrent que les verres stœchiométriques As_2Se_3 et $GeSe_2$ consistent en une phase majoritaire riche en Se, séparée d'une phase minoritaire compensatoire riche en Ge ou en As, c'est-à-dire qu'elles sont *séparées à l'échelle nanométrique*. Par ailleurs, les verres ternaires $Ge_x(As \text{ ou } P)_xSe_{1-2x}$ contenant des proportions égales d'éléments des groupes IV et V révèlent des tendances compositionnelles de $T_g(x)$ qui augmentent de façon monotone avec x ; il apparaît qu'ils polymérisent de manière croissante sur un large domaine de connectivité $2 < r < 2{,}8$ et sont homogènes. Dans ces verres ternaires, *la preuve expérimentale des transitions de rigidité est observée au voisinage de* $\bar{r} = 2.40$. La transition de rigidité aux alentours de $\bar{r} = 2.67$, dont on a pu précédemment faire état, peut être imputable à des effets de séparation de phase à l'échelle nanométrique. ***Pour citer cet article : P. Boolchand et al., C. R. Chimie 5 (2002) 713–724***

effets de séparation de phase à l'échelle nanométrique / transitions de rigidité / verres chalcogénures / Raman / Mössbauer

* *Correspondence and reprints.*
E-mail address: punit.boolchand@uc.edu (P. Boolchand).

1. Introduction

The notion of global connectivity has played a useful role to understand the physical behavior of network glasses and amorphous thin-films. The idea emerged in an embryonic form in the early seventies as material properties [1] of the chalcogenides were examined as a function of composition. However, it was not until the early eighties that a theoretical foundation evolved with the recognition that bonding interactions in covalent glasses form a hierarchy, and that nearest-neighbor valence interactions can serve as Lagrangian constraints [2]. This led to the evolution of a mean-field theory of elasticity [3] and the prediction [2, 3] of a solitary *floppy* to *rigid* phase transition in network glasses, when the number of such constraints/atom, n_c, increases to 3. These counting algorithms permit enumerating n_c in terms of the mean coordination number, $\bar{r}$, of a network, and lead to a threshold value of $\bar{r} = \bar{r}_c = 2.40$ at the rigidity transition first identified [2, 3] by J.C. Phillips and M.F. Thorpe.

In the past five years, new insights into elastic thresholds have emerged in chalcogenide glasses from *theory* [4] as well as *experiments* [5]. Specifically, Temperature Modulated Differential Scanning Calorimetry and Raman scattering have revealed [5] not *one* (transition) but actually *two* rigidity transitions as discussed elsewhere. The two transitions define the limits of an *intermediate phase* [6] that separates the *floppy* from the *stressed rigid* phase. It has lead to a structure based classification of glasses in terms of their elastic response: *floppy-intermediate-stressed rigid*. The novelty as well as challenge of the intermediate phase here is that it is a *non-mean-field* phase. This new classification is having consequences in a number of diverse fields, including protein folding [7], phase diagrams of high-Temperature Superconductors [8], and the phase transition associated with NP-complete problem [9] in computer science.

Nanoscale phase separation effects can give rise to pronounced changes in physical properties of network glasses such as molar volumes [10] and optical band gap [11] near $\bar{r} = 2.4$ and 2.67. The central issue at hand then is, how are we to distinguish *elastic effects* from *nanoscale phase separation ones*? In this work we provide guidance on phase separation effects in glasses. Compositional trends in physical properties of the chalcogenides suggest that rigidity transitions effects are clearly separated from nanoscale phase effects for transitions observed near $\bar{r} = 2.40$.

The use of the term nanoscale phase separation in this review is to denote networks that are, in general, partially polymerized with the size of the minority regions not to exceed 100 nm typically. Such glasses display a single glass-transition temperature T_g. These are to be contrasted from macroscopically heterogeneous glasses displaying bimodal T_gs in which the phases could extend to microns in size. This review is structured as follows. In section 2, we summarize ideas on the connection between T_g and network connectivity. In section 3, we provide thermal and spectroscopic evidence that shows As- and Ge–based stoichiometric chalcogenide glasses nanoscale phase separate near $\bar{r} = 2.40$ and 2.67, respectively. On the other hand, such effects are suppressed qualitatively due to chemical disorder in ternary (As or $P)_x Ge_x Se_{1-2x}$ glasses containing equal concentrations of the group IV and V elements. In these ternaries, rigidity transition effects are observed near $\bar{r} = 2.40$, as discussed in sections 4 and 5, respectively. However, the molecular origin of physical anomalies near $\bar{r} = 2.67$ is better understood as due to nanoscale phase separation rather than a rigidity transition associated with a dimensionality change as has been proposed [12].

2. Nanoscale phase separation and threshold behavior of T_g

One usually estimates the global connectivity of a network in terms of its mean coordination number, $\bar{r}$, by weighting the coordination numbers of constituent atoms in proportion to their concentrations in a network. Thus, for the case of the binary $As_x(Se \text{ or } S)_{1-x}$ glasses, the mean coordination number $\bar{r}$ becomes:

$$\bar{r} = x(r_{As}) + (1 - x)\, r_{Se} \qquad (1)$$

and taking the coordination numbers $r_{As} = 3$, and $r_{Se} = 2$, one obtains:

$$\bar{r}(x) = 2 + x \qquad (2)$$

The linear increase in $\bar{r}(x)$ (equation (2)) suggests that the global connectivity of these binary glasses increases monotonically with x. The mathematical construction however does not insure that such is the case in these binary glasses *at all x*. How are we then to decide if the global connectivity of a glass network continues to increase, or does the network actually nanoscale phase separate at some threshold concentration of As? In principle, the direct answer would appear to be to examine the molecular structure of glasses in diffraction or electron microscopy measurements. Unfortunately, even in crystalline solids detection of nanoscale phase separation effects by structure methods has proved to be rather difficult. In the case of disordered systems the approach poses formidable challenges. An alternative but well-grounded approach comes from examining compositional trends in the

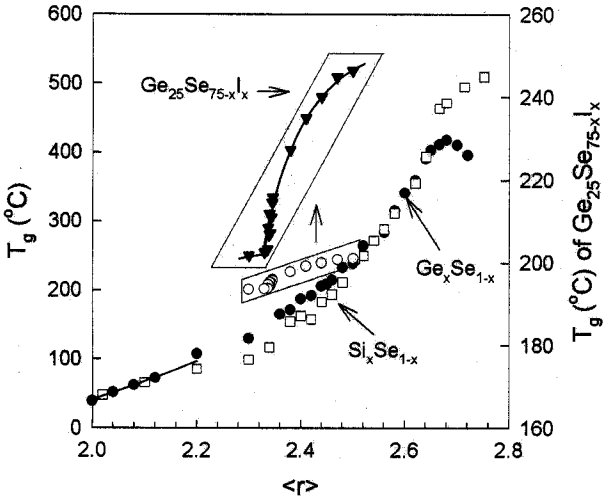

Fig. 1. Compositional trends in T_g in binary Si_xSe_{1-x} (□) and Ge_xSe_{1-x} glasses (●), and ternary $Ge_{25}Se_{75-x}I_x$ glasses (○ or ▼) plotted as a function of r, taken from refs [5], [54], and [58], respectively. The sharp decrease in T_g for the ternary (inset) occurs near $r = 2.34$, the rigidity transition.

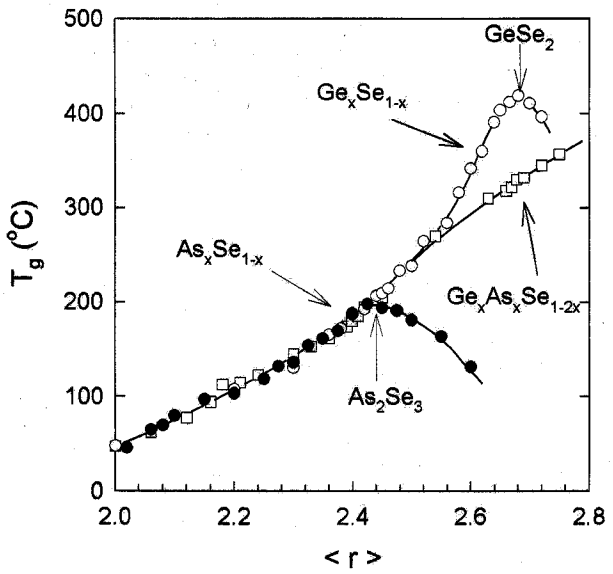

Fig. 2. Compositional trends in T_g in As_xSe_{1-x} (●), Ge_xSe_{1-x} (○) and $As_xGe_xSe_{1-2x}$ (□) glasses plotted as a function of r, the mean coordination number taken from refs [19], [54], and [39], respectively.

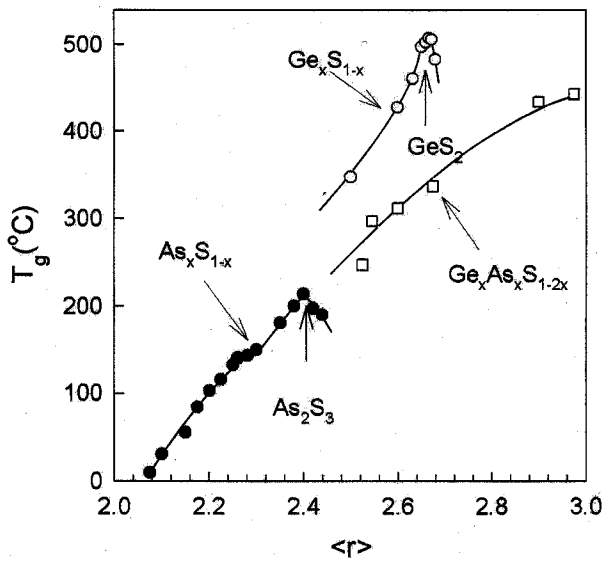

Fig. 3. Compositional trends in T_g in As_xS_{1-x} (●), Ge_xS_{1-x} (○) and $As_xGe_xS_{1-2x}$ (□) glasses plotted as a function of r, the mean coordination number taken from refs [20], [38], and [41], respectively. The T_g results on the ternary are from DSC measurements taken from ref. [41], while the other set of results are from MDSC.

glass-transition temperature, $T_g(x)$. Although T_g of a glass is widely ascribed to kinetics [13] of cooling, the experimental fact remains that alloying or glass structure effects produce far larger changes in T_g than kinetic ones.

There is growing recognition that T_g is an excellent measure of global connectivity of a glass network. The idea forms the basis of stochastic agglomeration theory [14, 15], which permits calculating changes in T_g as a function of network cross-linking or chemical composition. The theory has successfully provided a formal derivation [15] of the Gibbs–Di Marzio phenomenological relation [16] that describes increases of T_g in polymers as a function of cross-linking. In the stochastic limit, the results of these combinatorial calculations are found to be in excellent agreement with results on the group IV selenides (Fig. 1). The observed slope, dT_g/dx, in both Si_xSe_{1-x} and Ge_xSe_{1-x} glasses at low x (< 0.10) where agglomeration effects are considered to be stochastic, is in excellent accord with the parameter-free value of this slope,

$$dT_g/dx = T_g(\mathrm{Se})/\ln 2 \qquad (3)$$

predicted [15] by stochastic agglomeration theory.

Experiments on As_xSe_{1-x} [17–19] (Fig. 2) and As_xS_{1-x} [17, 20, 21] (Fig. 3) glasses show that in the $0 < x < 0.40$ range, $T_g(x)$ increases monotonically with x. We can understand the behavior in terms of the Se-chain network becoming progressively more connected as As-centered pyramidal units emerge. The process of cross-linking Se chains clearly saturates near $x = 0.40$. At higher x (> 0.40), T_gs are found to decrease progressively, suggesting that now the global connectivity of the glass network apparently *decreases* as the As content of the glasses increases. The As–As bonds that appear in the network at $x > 0.38$, apparently *do not form part* of the backbone of the network. Raman scattering experiments in both As–Se [22] and As–S [20] glasses show the evolution of As_4Se_4 and As_4S_4 monomers in corresponding glasses once $x > 0.38$. These monomers grow in concentration

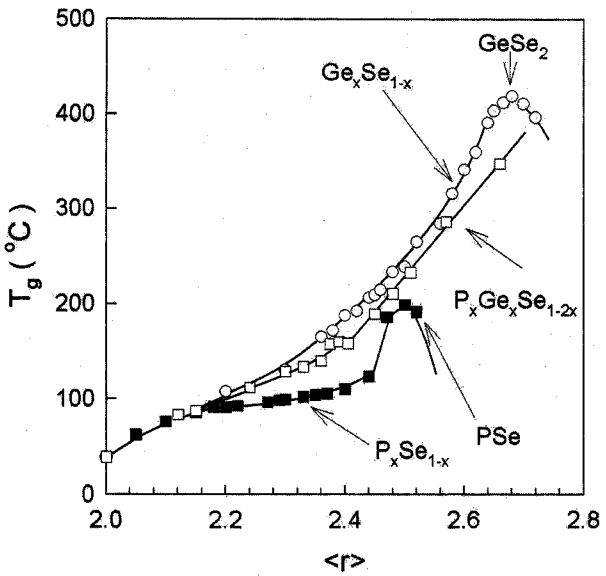

Fig. 4. Compositional trends in T_g in P_xSe_{1-x} (■), Ge_xSe_{1-x} (○) and $P_xGe_xSe_{1-2x}$ (□) glasses plotted as a function of r, the mean coordination number taken from refs [24], [54], and [43], respectively.

at the expense of the backbone of the network, thus lowering the connectivity of the network globally. We thus arrive at the notion that the microscopic origin for the reduction of T_g at $x > 0.40$ is *nanoscale phase separation* of the network. Indeed the existence of a threshold of T_g near $x = 0.40$ constitutes evidence of nanoscale phase separation in both these binary glasses.

A similar result is observed in binary P_xSe_{1-x} glasses [23, 24], where T_gs are found to increase in the $0 < x < 0.50$ range and then to plummet rather sharply once $x > 0.50$ (Fig. 4) as P_4Se_3 monomers emerge in the glasses. Not only do T_gs decline to room temperature and below, but the glass forming tendency is found to nearly vanish near $x = 0.57$, when a crystalline molecular solid composed of P_4Se_3 cages is formed even upon a water quench of melts.

2.1. T_g and the role of chemical bond strengths

A correlation between compositional trends in T_g and average chemical bond strengths in chalcogenide glasses was noted by Tichy and Ticha [25]. Chemical bond strengths play a scaling role in determining T_gs, when comparing networks having the *same global connectivity* ($\bar{r}$), such as GeS_2 with $GeSe_2$, or As_2S_3 with As_2Se_3. However, such chemical considerations *alone* cannot account for the observed changes in T_g as a function of $\bar{r}$, which are *structure-related*. Two examples would serve to make the case. In binary As–S glasses $T_g(x)$ are found to increase [20] monotonically (Fig. 3) with x in the $0 < x < 0.40$ range. Pauling single bond strength [26] of a S–S bond of 50.9 kcal mol^{-1} *exceeds* that of As–S single bond of 47.25 kcal mol^{-1}. Indeed, if average bond strengths alone were to determine T_gs of As_xS_{1-x} glasses as has been suggested [25], *one would expect* T_g to *decrease with the As content* x. On the other hand, the observed *increase* of T_g with x is precisely the behavior one expects as the S-chain network is progressively cross-linked by As resulting in an increase of the global connectivity in the $0 < x < 0.40$ range.

Fig. 1 compares compositional trends in T_g in the Ge–Se binary [27] with the Si–Se one [28]. The glaring difference between these trends is the *presence* of a threshold in T_g near $x = 1/3$ or $\bar{r} = 2.67$ in the Ge–Se binary, but the *absence* of it in the Si–Se binary. The Pauling single bond strength [26] of a Ge–Se bond exceeds that of a Ge–Ge bond by 11.5 kcal mol^{-1}, while that of a Si–Se bond exceeds that of a Si–Si bond by 9.2 kcal mol^{-1}. If average bond strengths alone were the factor controlling compositional trends in T_g, one would be hard pressed to understand why T_gs decline at $x > 1/3$ in the Ge–Se binary, but increase at $x > 1/3$ in the Si–Se binary, when weaker homopolar bonds (Si–Si, Ge–Ge) emerge in both systems.

The T_g trends above are precisely the ones expected if Ge–Ge bonds were to *segregate* [29] from the Ge–Se backbone to nucleate a separate Ge-rich nanophase, and thus lower the global connectivity, while Si–Si bonds were to form *part* [30] of the Si–Se backbone and increase its global connectivity, and thus T_g of the glasses. Si–Se melts at $x > 1/3$ possess astronomically high viscosities [30] understandably because of the fully polymerized nature of the underlying backbones. The case of the Si_xSe_{1-x} binary glass system at $x > 1/3$, is the *exception that proves the rule* that T_gs are a good representation of network connectivity with chemical bond strengths playing the role of scaling these numbers between networks of similar global connectivities.

2.2. The vibration iso-coordination rule

Inelastic neutron scattering studies on ternary $As_xGe_ySe_{1-x-y}$ glasses have proved an elegant probe of the low frequency vibrational density of states (VDOS) [31, 32]. The excitations in the 5 meV region are usually identified with floppy modes [32] in undercoordinated networks. Effey and Cappelletti have found [33] scattering strength of these excitations to be strictly controlled by the global connectivities of glasses as measured by their mean coordination number, $\bar{r} = 3x + 4y + 2(1 - x - y)$, and to be independent of chemical compositions so long as $\bar{r} < 2.40$. A parallel result was noted for vibrational lifetime of a H_2O guest molecule in these glasses, which increased

[34] monotonically with $\bar{r}$, regardless of chemical composition. These results support the notion that at low r (< 2.4), the Se-rich glasses are fully polymerized and continue to be so as the group IV and V elements are added to increase global connectivity of the backbone.

A striking exception to this rule emerged in binary As_xSe_{1-x} glasses at $x = 0.6$, for which the low frequency VDOS are found to be characteristic of a floppy glass ($\bar{r} = 2.35$) even though the chemical composition suggests a rigid glass ($\bar{r} = 2.60$). In the neutron VDOS [32], sharp modes are observed between 10 and 20 meV. These modes have contributions from characteristic As-rich clusters (As_4Se_4 and As_4Se_3) and amorphous As, for which confirmation is given by FT-Raman measurements [22, 35, 36]. The sharpness of the modes suggests that these As-rich clusters are decoupled from the backbone. The exception to the vibration isocoordination rule falls in line with the sharply reduced glass transition of this composition [32, 19]. These results are consistent with nanoscale phase separation of this As-rich glass.

3. Stoichiometric binary chalcogenide glasses and nanoscale phase separation effects

The threshold behavior in T_g observed in binary Ge_ySe_{1-y} and As_xSe_{1-x} glasses, near $y = 1/3$ and $x = 2/5$, respectively, as discussed in section 2, we therefore take as evidence for nanoscale phase separation of these stoichiometric glasses. Insights into the molecular structures responsible for this phase separation emerge from Raman and Mössbauer spectroscopy results [20, 29].

In binary Ge–Se glasses, Raman scattering measurements (Fig. 5a) show [29] evolution of a mode at 178 cm^{-1} first emerges [29] near a threshold composition of $x = 0.32$. The mode is identified with presence of ethanelike $Ge_2(Se_{1/2})_6$ units. In ^{119}Sn Mössbauer spectroscopy (Fig. 5b), a non-tetrahedral site is found to first emerge near the same threshold of $x = 0.32$. The site is assigned to Sn present in ethanelike units. The slope, dT_g/dx, decreases sharply once these non-tetrahedral local units first appear in the network. This is not a coincidence. The reduction in the slope dT_g/dx, once these Ge–Ge bonds first appear in the glass suggests that these bonds *do not form part of the backbone*, in other words the ethanelike units form a separate nanophase from the backbone. The backbone here comprises of corner- and edge sharing tetrahedral Ge $(Se_{1/2})_4$ units. A parallel result is found in Ge_xS_{1-x} glasses [37] near $x = 0.32$, as discussed in recent work [38].

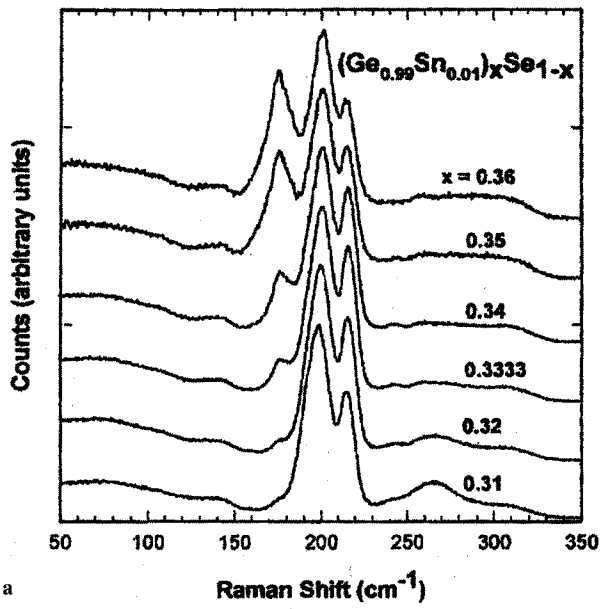

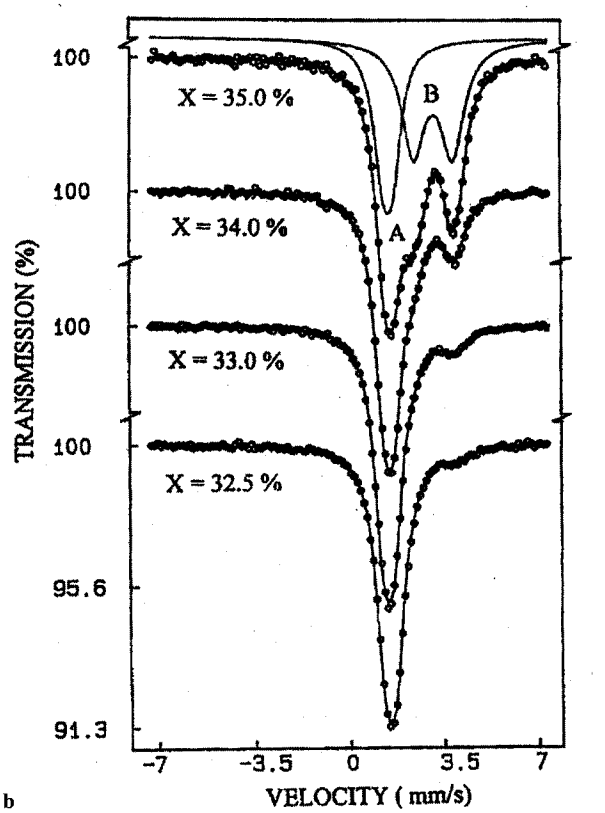

Fig. 5. (a) Raman scattering (b) and ^{119}Sn Mössbauer spectra of $(Ge_{0.99}Sn_{0.01})_xSe_{1-x}$ glasses showing respectively evolution of the 178–cm^{-1} mode and the B-site quadrupole doublet as a function of x starting from $x = 0.32$. Results taken from ref. [?]. Both spectroscopic features are ascribed to ethanelike units populated in the network.

Raman scattering in As_xS_{1-x} glasses near $x = 2/5$ taken from ref. [20] are reproduced in Fig. 6. Noteworthy in the lineshapes is the emergence of sharp

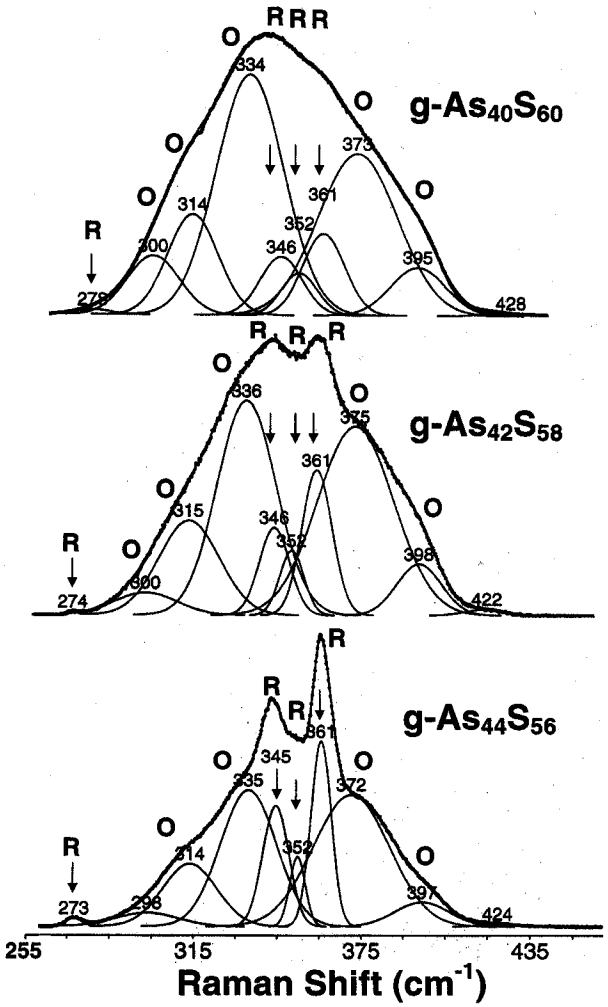

Fig. 6. Ramanline deconvolution of bulk As_xS_{1-x} glasses at indicated compositions showing modes of orpimentlike (○) and Realgarlike (R) phases taken from ref. [29]. The spectra were obtained using 647-nm excitation in a macro-Raman configuration at room temperature.

modes labeled R once the As content exceeds approximately of 0.38. These modes are identified with Realgarlike modes, i.e. As_4S_4 monomers, that apparently nucleate in the binary glasses once x exceeds 0.38. The sharpness of these Realgar modes is due to the fact that these units are decoupled from the backbone, suggesting that the stoichiometric glass is nanoscale phase separated.

4. Absence of nanoscale phase separation in ternary $Ge_x(As\ or\ P)_xSe_{1-2x}$ glasses

The titled ternary glasses are of general interest because compositional trends in $T_g(x)$ in these systems (Figs. 2 and 4) display a *monotonic increase* [39, 40] *with* x, even when $\bar{r} > 2.67$. The behavior is in sharp contrast to the threshold in T_g observed [19, 29] in corresponding binary (As–Se, Ge–Se) glasses. A parallel T_g result is found [40] in the Ge–As–S ternary when compared to corresponding binary glasses (Fig. 3). In these ternary glass systems, there is an equal concentration of the group IV and V additives, which leads to a mix of As-centered pyramids with Ge-centered tetrahedra. The mix promotes chemical disorder and suppresses *nanoscale phase separation effects* even as the additive concentration increases as reflected in the monotonic increase of T_g. These glass systems are thus ideal to examine rigidity percolation effects.

The $P_xGe_xSe_{1-2x}$ ternary displays compositional trends in T_g that show an *almost linear increase* in the $2.40 < \bar{r} < 2.80$ range [42, 43] suggestive of increased global connectivity as a function of $\bar{r}$ even at $\bar{r} > 2.67$. Aspects of glass molecular structure that lead to such a behavior are currently less well understood. The P-centered structures in these glasses were probed in ^{31}P NMR measurements [42]. The subject is currently under investigation by Raman and Mössbauer spectroscopy measurements [43] that are providing valuable information on the nature of the Ge-centered and Se-centered structures. There are striking similarities as well as glaring differences in the structure of the P-based ternary glasses from the corresponding As-based ones. For example, in MDSC measurements of the P-based glasses, one observes a sub-T_g endotherm [43], which is not observed in corresponding As-based glasses. These aspects of structure are currently under investigation.

Vibrational temperatures of ^{119}Sn sites in ternary As–Ge–Se glasses

We have examined Ge-centered local structures in the As-Ge–Se ternary in Raman scattering and ^{119}Sn Mössbauer spectroscopy [44] measurements. In Raman scattering, one observes modes of corner-sharing and edge-sharing $Ge(Se_{1/2})_4$ tetrahedra to emerge with increasing x. At higher x ($x > 0.21$) modes of ethanelike Ge–Ge units manifest in the lineshape. In Mössbauer spectroscopy [44], tetrahedral Sn sites (labeled A) appear in the Se-rich $0 < x < 0.18$ glasses, but non-tetrahedral Sn-sites (labeled B) to first appear once $x > 0.18$ in Ge-rich glasses as shown in Fig. 7. These non-tetrahedral sites constitute signature of Ge–Ge bonds in the network [45]. Simple counting arguments reveal that a chemical threshold occurs at $x_c = 0.182$ above which Ge–Ge bonds are expected.

Lamb–Mössbauer factors of the A and B sites have been measured [44] by recording spectra of glasses at $x > 0.18$ as a function of temperature. From these

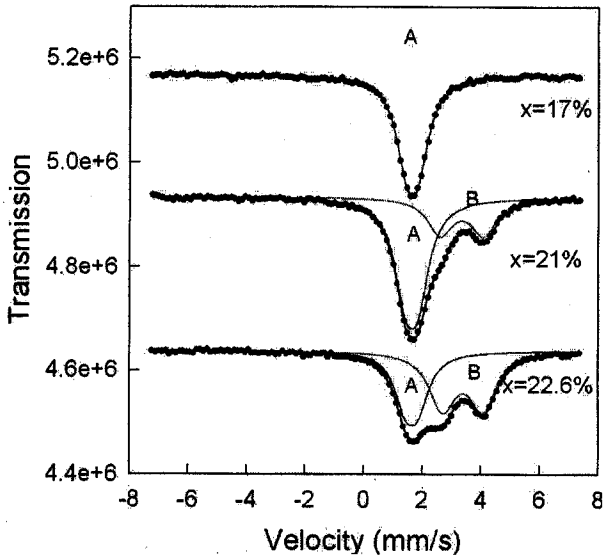

Fig. 7. ^{119}Sn Mössbauer spectra of ternary $Ge_xAs_xSe_{1-2x}$ glasses at indicated compositions x, showing tetrahedrally coordinated Sn sites (A) and non-tetrahedral sites (B), when $x > 0.18$. The B sites represent signature of Ge–Ge bonds emerging in the network. Figure taken from ref. [29].

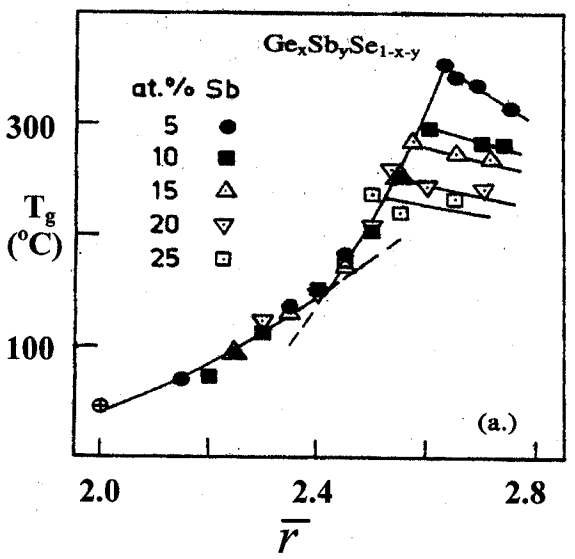

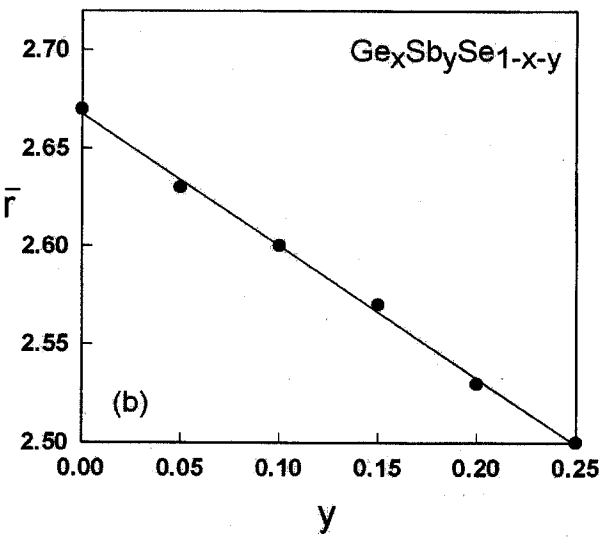

Fig. 8. **a.** $T_g(\bar{r})$ variation in ternary $Ge_xSb_ySe_{1-x-y}$ glasses showing the threshold behavior in T_gs to systematically move to lower $\bar{r}$ values as the indicated Sb concentrations (y) are increased. The figure is taken from ref. [47]. **b.** The predicted variation in the threshold value of $\bar{r}$ from a nanoscale phase separated model developed here and the observed threshold value of $\bar{r}$ taken from ref. [47].

results we obtain the vibrational temperature (effective Debye Temperature) of the A and B sites. Results of these experiments show that their vibrational temperatures are $\theta_D^A = 125 \pm 2$ K and $\theta_D^B = 110 \pm 2$ K i.e., about 15 K apart. We had performed similar measurements in binary Ge_xSe_{1-x} glasses earlier [32, 46], and found vibrational temperatures of these two sites, $\theta_D^A = 130 \pm 2$ K, and $\theta_D^B = 100 \pm 2$ K, to be 30 K apart in these nanoscale phase separated materials. Thus, vibrational temperatures of chemically inequivalent sites in nanoscale-phase separated glasses differ significantly more than in homogeneous glasses reflecting the intrinsic heterogeneity of the former systems.

5. Alloying behavior of Sb and As additives in chalcogenide glasses contrasted

New insights into the chemical alloying behavior of pnictide additives in chalcogenide glasses have emerged from the compositional variation of Glass-transition temperatures. In this section we discuss the alloying behavior of Sb and separately As in Ge_xSe_{1-x} glasses.

5.1. Glass-transition temperature variation in the $Ge_xSb_ySe_{1-x-y}$ ternary

In an impressive set of measurements of T_g and molar volumes in the titled ternary, Mahadevan and Giridhar [47] found that the threshold behavior of $T_g(\bar{r})$ near $\bar{r} = 2.67$ observed at $y = 0$, i.e., binary Ge_xSe_{1-x} glasses (Fig. 2), shifts rather systematically (Fig. 8a) to lower values of $\bar{r}$ as the Sb content (y) of titled ternary glasses increases in the $0 < y < 0.25$ range. The existence of this threshold shift suggests nanoscale phase separation must occur. For a trivalent pnictide on strictly chemical grounds, one can always write:

$$Ge_x Sb_y Se_{1-x-y} = (5\,y/2)\,(Sb_{2/5} Se_{3/5}) + Ge_x Se_{1-x-5y/2} \quad (4)$$

In the present case, however, the first and second terms on the right hand side of equation (4) describe, respectively, the Sb-rich nanophase that segregates from the base glass phase. Because of such separation, the base glass can nanoscale phase separate [29] when the Ge/Se stoichiometry ratio exceeds the threshold value of ½, i.e.:

$$x/(1 - x - 5\,y/2) = 1/2 \quad (5)$$

Thus, for a given Sb content (y), equation (5) serves to define a critical mean coordination number:

$$\bar{r}_c = 2 + 2\,x_c + y = (8 - 2\,y)/3 \quad (6)$$

when the ternary glass is expected to display a local maximum in T_g. In Fig. 8b, the straight line represents a plot of equation 6, while the data points are the observed thresholds reported [47] by Mahadevan and Giridhar. The correlation between theory and experiments is excellent. The central message is that in the present ternary the additive segregates into an Sb-rich nanophase (equation (4)) soaking Se from the base glass to eventually drive the base glass to phase separate as well.

5.2. Glass-transition temperature variation in the $Ge_xAs_ySe_{1-x-y}$ ternary

A very different physical picture of alloying As as opposed to Sb in Ge–Se glasses emerges from T_g trends of the $Ge_xAs_ySe_{1-x-y}$ ternary. The threshold behavior of T_gs so characteristic [29] of the base glass (Ge–Se) near $\bar{r} = 2.67$, is no longer observed when as little as 5 atomic percent of As is alloyed, as shown in Fig. 9. The results of Fig. 9 taken from ref. [47] are based on the work of Borisova [48] and Frischat [49]. These $T_g(\bar{r})$ trends suggest that $As(Se_{1/2})_3$ pyramids now *mix on a molecular scale with corner- and edge-sharing* $Ge(Se_{1/2})_4$ *tetrahedra, and* suppress nanoscale phase separation of the backbone. Ge–Ge bonds must still form at high $\bar{r}$, but they apparently do so as part of the main backbone, as noted earlier (section 4) for the case when $x = y$, in the Ge–As–Se ternary.

With increasing As concentration y in the Ge–As–Se ternary, one also notes that the T_gs increase (Fig. 9), but more slowly with r near 2.67, i.e. the slope $dT_g/d\bar{r}$ decreases. Important insights into the slopes dT_g/dr emerge from the stochastic agglomeration theory [14], which relates these to the number of ways building blocks (tetrahedra and pyramids) can agglomerate. Specifically, if there are several types of building blocks that can couple in many ways, the underlying entropy of mixing increases, and the calculations reveal [50] the slope dT_g/dr to invariably decrease. The pattern is also observed in binary glasses (Fig. 1), when one contrasts results on the two families of group IV selenides. For example, the slope near $\bar{r} = 2.30$ for Si_xSe_{1-x} glass is less than for Ge_xSe_{1-x} glasses, probably because of a substantially larger concentration of edge-sharing tetrahedra in the Si-bearing glasses than in the Ge-bearing ones.

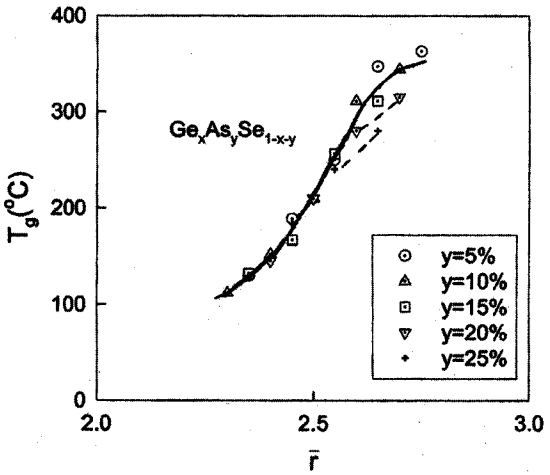

Fig. 9. $T_g(\bar{r})$ variation in ternary $Ge_xAs_ySe_{1-x-y}$ glasses taken from the work of Z.U. Borisova [48].

6. Rigidity transitions in network glasses

One of the success stories to emerge in glass science in the past two decades is the existence of elastic phase transitions as a function of connectivity of networks. These phase transitions have led to a structure based classification of glasses in terms of their elastic response [4, 6] as *floppy-intermediate- stressed rigid.*

6.1. Discovery of the intermediate phase

Although the existence of *floppy* and *rigid* phases was recognized starting in the mid eighties [32, 51, 52, 53], it was not until 1999 that experimental evidence for intermediate phases evolved [5, 28, 54]. These phases evolve in between floppy ($n_c < 3$) and stressed rigid ($n_c > 3$) phases, and their widths provide a measure of the degree of self-organization of a glass network. The widths of Intermediate Phases are apparently controlled by local and medium range structures that are stress-free. These phases were first observed in Raman scattering experiments on IV–VI binary glasses [27, 28, 54], wherein mode frequency (squared) variations as a function of $\bar{r}$ display distinct power-laws.

An important development in identification of intermediate phases has been the application of T-modulated Differential Scanning Calorimetry (MDSC) [55, 56]. The method permits deconvoluting the heat flow endotherm near T_g into two parts, a *reversing heat flow* and a *non-reversing heat flow.* The reversing heat flow is the fraction of the heat flow that tracks the programmed T-modulations and shows a text book glass transition on a flat baseline, independent of the instrument baseline. It permits a reliable *scan rate* and *thermal history* independent measurement of T_g. All (MDSC) T_g results reported in Figs. 1–4 were obtained from the inflexion point of the reversing heat flow using a model 2920 unit from TA Instruments, Incorporated at 3 °C min^{-1} scan rate and 1 °C/100 s modulation rate. In these scans, the non-reversing heat flow signal usually displays a peak as a precursor to the actual glass transition. In fully relaxed samples, the area under the peak provides the latent heat of melting of a glass and will henceforth be noted as the non-reversing heat.

The novelty of the intermediate phase is that *mean-field theories* cannot access it [4]. It is a rigid but stress-free phase of a glass. Glasses in the intermediate phase possess some very unusual physical properties including the near *absence* of a latent heat of melting. In other words, glasses ($T < T_g$) in these phases possess a configurational entropy that is nearly the same as in corresponding melts ($T > T_g$). This is revealed by the near *absence* of the non-reversing heat flow in MDSC measurements. Experiments on several glass systems have now been documented, and the results show the *optical elastic thresholds* to coincide [28, 54] with the *thermal ones.* To keep our discussion brief, we will therefore restrict to thermal thresholds, which can thus serve as a convenient probe of the rigidity transitions in glasses.

6.2. Thermally reversing windows in network glasses and rigidity transitions

Compositional trends of the non-reversing heat flow in binary Si_xSe_{1-x} [28] and ternary $Ge_{0.25}S_{0.75-y}I_y$ [57] glasses appear in Fig. 10a. Noteworthy in these trends is the squarewell-like behavior observed in the binary glass. The intermediate phase here extends from $x_c(1) = 0.20$, or $\bar{r}_c(1) = 2.40$ to $x_c(2) = 0.26$ or $\bar{r}_c(2) = 2.52$, with glass compositions at $x < x_c(1)$ reckoned as floppy, while those at $x > x_c(2)$ as stressed rigid. The situation is replicated in the companion Ge_xSe_{1-x} glasses as discussed [54] elsewhere.

The case of the Ge–S–I ternary [57] is profound, because in this case the upper and lower bounds of the intermediate phase coincide, giving rise to a narrow peak in the non-reversing heat centered near $r = 2.34$. This is a remarkable result because it corresponds exactly to the value of $\bar{r}$ where mean-field theory predicts the floppy to rigid transition to occur. A parallel circumstance occurs in the Ge–Se–I ternary [58]. In Fig. 1, we note that T_gs in the Ge–Se–I ternary show a precipitous drop near $\bar{r} = 2.34$, signaling the sharp rigid to floppy transition. The agreement between theory and experiment here is unparalleled in glass science. It raises the broader issue why does mean-field theory work so well in these ternary glasses when it completely breaks down in binary Ge–Se, and Si–Se glasses. The answer rests in the recognition that Iodine alloying randomly cuts S or Se bridges of the backbone, and the replacement inhibits the medium-range structure of the backbone in the form of rings to form. Constraint counting algorithms do not distinguish between S and Se in these glasses. Taken together, these results serve to demonstrate that the physical origin of the observed effects must indeed stem from rigidity effects.

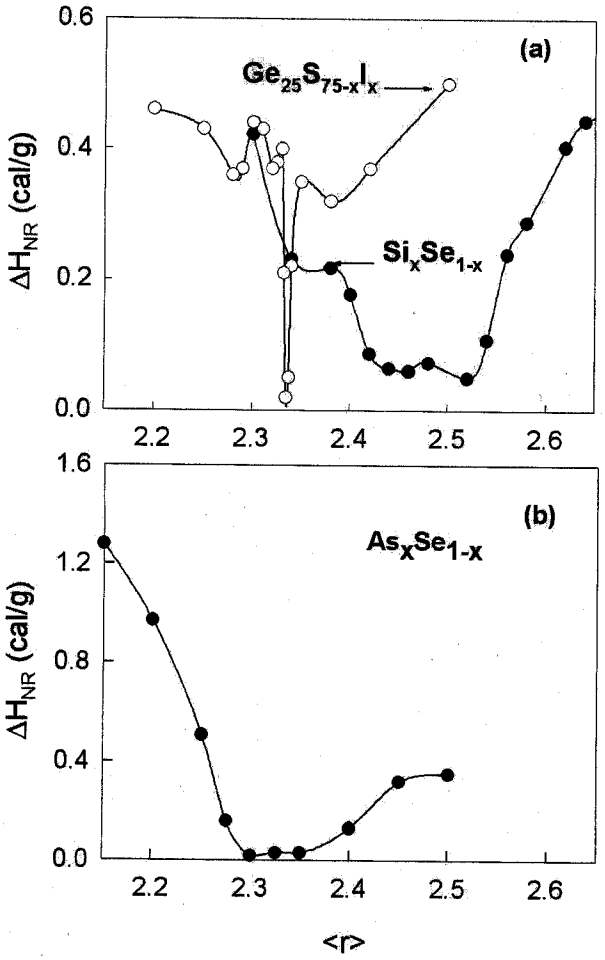

Fig. 10. Compositional trends of the non-reversing heat flow in (**a**) the Si_xSe_{1-x} binary, the $Ge_{0.25}Se_{0.75-y}I_y$ ternary, and (**b**) the As_xSe_{1-x} binary glasses, revealing thermally reversing windows of varying widths and centroid. These windows are identified with intermediate phases.

Compositional trends in the non-reversing heat flow in binary As_xSe_{1-x} glasses [19] appear in Fig. 10b. Here the intermediate phase is localized between $x_c(1) = 0.27$ or $\bar{r}_c(1) = 2.27$ and $x_c(2) = 0.38$ or $\bar{r}_c(2) = 2.38$. This is also a fascinating result because it opens new ground. The result is inconsistent [19, 59] with the conventional picture of only pyramidal As-centered local structures present in the molecular structure of these Se-rich glasses. The downshift of the window onset to $\bar{r}_c(1) = 2.27$ that we have suggested [19] is consistent with inclusion of quasi-tetrahedral As-centered local $Se{=}As(Se_{1/2})_3$ units in the structure of these glasses. In this case, MDSC measurements through the non-reversing heat flow have yielded a new feature of local structure that was apparently not recognized in earlier structure studies.

In all the three cases discussed above, it is noteworthy that rigidity transitions occur at ranges of $\bar{r}$, below the regime where nanoscale phase separation effects manifest. These rigidity transitions are thus quite distinct from nanoscale phase separation effects.

6.3. The very special case of ternary $As_xGe_xSe_{1-2x}$ glasses

The glass-forming region [48] in the As–Ge–Se ternary appears in Fig. 11. The hashed marked region shows the opening of the intermediate phase in between the stressed rigid and the floppy phases. The region straddles compositions near $\bar{r} = 2.40$ shown as a broken tie-line connecting the binary compositions, $GeSe_4$ with As_2Se_3. Also shown in Fig. 11 are the regions (shaded) of glass formation where nanoscale phase separation effects manifest. Such effects are largely localized along the binary rich compositions, and for that reason even ternary compositions that are either As-rich or Ge-rich display features characteristic of nanoscale-separated glasses.

Compositional trends in the non-reversing heat flow in ternary $As_xGe_xSe_{1-2x}$ glasses [39] appear in Fig. 12. The intermediate phase in this case extends from $x_c(1) = 0.10$ or $r_c(1) = 2.30$ to $x_c(2) = 0.155$ or $r_c(2) = 2.46$. This is a rather broad range, and it encompasses the intermediate phases of both the Ge–Se and the As–Se binary glasses. The width of the intermediate phase suggested from these thermal measurements, has recently been refined from the more precise Raman scattering measurements [44] and will be discussed in a forthcoming publication.

6.4. Electrical and phonon transport in ternary $Ge_xAs_{0.40-x}Se_{0.60}$ glasses

Several groups have examined thermal and electrical transport in ternary $Ge_xAs_{0.40-x}Se_{0.60}$ glasses and amorphous thin films, and rather complete results are now available for discussion. To orient the reader, it

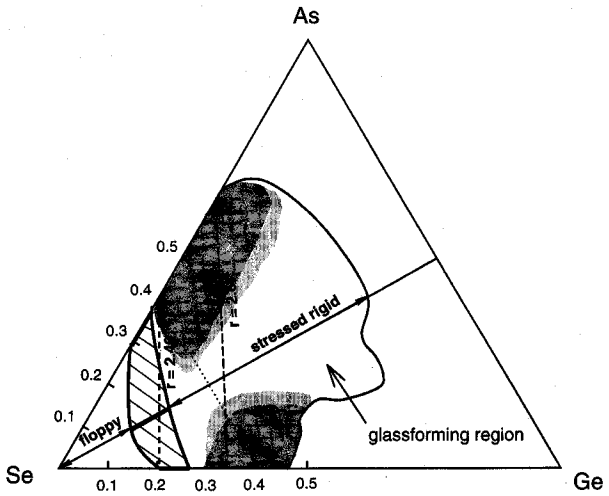

Fig. 11. Glass-forming region in the As–Ge–Se ternary taken from ref. [48]. The hashed marked region straddling the isocoordination line $r = 2.4$ represents the evolution of the intermediate phase in between the floppy (left) and the stressed rigid phase (right). The shaded regions reflect compositions where glass networks are viewed to be nanoscale phase separated. These regions overlap with the $r = 2.67$ isocoordination line near the Ge-rich and As-rich compositions. The dotted line describes the $As_{0.4}Se_{0.6}$ join to $Ge_{0.4}Se_{0.6}$.

might be well to mention that this ternary joins the two binary end member compositions, $As_{0.40}Se_{0.60}$ and $Ge_{0.40}Se_{0.60}$, and furthermore it intersects the $Ge_xAs_xSe_{1-2x}$ ternary (Fig. 11) of interest at right angles at $x = 0.20$. The line composed of points spans compositions in this ternary, as shown in Fig. 11.

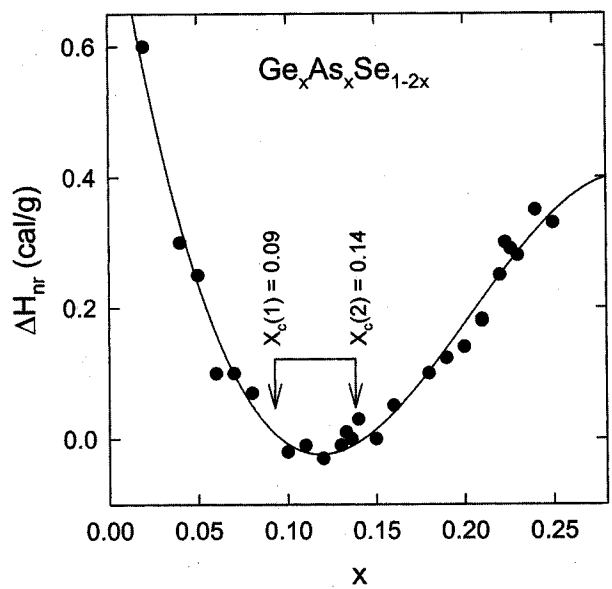

Fig. 12. Compositional trends in non-reversing heat flow in ternary $Ge_xAs_xSe_{1-2x}$ glasses revealing a wide thermally reversing window with an onset near $x_c(1) = 0.09$ or $r_c(1) = 2.27$ and an end near $x_c(2) = 0.14$ or $r_c(2) = 2.42$. There is no evidence of any anomalies near $r = 2.67$ or $x = 0.22$.

Thermal diffusivities, ($\alpha(x)$), of bulk $Ge_xAs_{0.40-x}Se_{0.60}$ glasses and their S-counterparts were examined over the $0 < x < 0.40$ range by Velinov et al. [60]. They showed $\alpha(x)$ to display a global minimum near $x = 0.15$ for the selenide glasses, and near $x = 0.18$ for the sulfide glasses. Dark electrical conductivities, $\sigma_d(x)$, in carefully annealed selenide thin-films over the full range ($0 < x < 0.40$) of compositions were studied by Nesheva and Skordeva [61]. Their results show a rather spectacular narrowly defined deep global minimum in $\sigma_d(x)$ near $x = 0.22$.

The end member compositions of the $Ge_xAs_{0.40-x}Se_{0.60}$ ternary are intrinsically nanoscale phase separated (Fig. 11). The molecular structure of $Ge_{0.40}Se_{0.60}$ glass inferred from Raman scattering and Mössbauer spectroscopy measurements has shown [46, 62] that it consists of two nanophases, an ethanelike phase and a distorted rocksalt phase. In section 2, we have discussed the case of nanoscale phase separation in $As_{40}Se_{60}$ glass. On the other hand, a glass composition at the midpoint, i.e., $x = 0.20$, which also forms part of the $Ge_xAs_xSe_{1-2x}$ ternary, is rather special because it is *spatially homogeneous*. The most natural interpretation of the global minima in both $\alpha(x)$ and $\sigma_d(x)$ near $x = 0.20$, or $\bar{r} = 2.60$ is that it represents phonon and charge–transport *localization* in these fully polymerized networks. Carrier transport in glass compositions on either side of the global minimum is aided by the presence of internal surfaces in heterogeneous (nanoscale phase separated) structures. This is akin to increased diffusion of carriers at grain boundaries in a polycrystalline material as opposed to a single crystal. These results highlight the important role of glass structure morphology (homogeneous versus heterogeneous), on transport measurements, also noted earlier in work [63, 64] on chalcogenides.

The experimental evidence of a rigidity transition due to a dimensional regression from 2d to 3d, as suggested by Keiji Tanaka [12], would be best observed in a glass system, such as the $Ge_xAs_xSe_{1-2x}$ ternary where *nanoscale phase separation effects are absent*. Neither Raman scattering nor MDSC results provide evidence of anomalies near $\bar{r} = 2.67$ in the present ternary [39]. The present results do not provide evidence of a rigidity transition due to a dimensionality change. Many of the glass systems where such an effect has been claimed [12, 47, 60, 61], upon close examination, are all found to be nanoscale phase separated [65]. Finally, independent evidence for onset of nanophase separation in Ge–Se glasses at $\bar{r} > 2.67$ has been obtained by T-dependent Raman measurements recently [66]. Neutron structure factors of $GeSe_2$ glass [67] that have been analyzed by molecular dynamic simulations [68, 69] have to date not considered these nanoscale phase separation effects. Alternatively, structure studies on present ternary glasses that apparently do not phase separate, would appear to be rather attractive systems to investigate in future.

7. Concluding remarks

Compositional trends in T_g provide valuable insights into the molecular structure of network glasses. Ge–Se based glasses and their S counterparts, at low mean coordination number $\bar{r} < 2.60$, are usually fully polymerized, but nanoscale phase separate at higher $\bar{r}$ (> 2.60) glasses. As–Se based glasses and their S analogues are usually fully polymerized at $\bar{r} < 2.40$, but nanoscale phase separate at higher $\bar{r}$ (> 2.40). On the other hand, ternary $Ge_xAs_xSe_{1-2x}$ glasses containing equal concentrations of the group IV and group V additives are quite special, they appear to be fully polymerized to reasonably high values of $\bar{r}$ (> 3.0) and are attractive systems to examine elastic thresholds in glasses. Raman scattering and T-modulated Differential Scanning Calorimetric measurements in such spatially homogeneous networks reveal in general the presence of two elastic thresholds near $\bar{r} = 2.40$, but no evidence of a rigidity transition near $\bar{r} = 2.67$ that could be due to dimensionality change.

Acknowledgements. It is a pleasure to acknowledge discussions with M. Micoulaut, D. McDaniel and R. Kerner during the course of this work. The assistance of the late Professor Ernst Franke in providing facilities to synthesize glasses is acknowledged. This work is supported by US National Science Foundation grant DMR-01-01808.

References

[1] J.P. DeNeufville, H.K. Rockstad, in: J. Stuke, W. Brenig (Eds.), Amorphous Liquid Semiconductors, Taylor and Francis Ltd, London, 1974, pp. 419.

[2] J.C. Phillips, J. Non-Cryst. Solids 34 (1979) 153.

[3] M.F. Thorpe, J. Non-Cryst. Solids 57 (1983) 355.

[4] M.F. Thorpe, D.J. Jacobs, M.V. Chubynski, J.C. Phillips, J. Non-Cryst. Solids 266–269 (2000) 859.

[5] D. Selvanathan, W.J. Bresser, P. Boolchand, Phys. Rev. B 61 (2000) 15061.

[6] P. Boolchand, D.G. Georgiev, B. Goodman, J. Optoelectron. Adv. Mater. 3 (2001) 703.

[7] A.J. Rader, B.M. Hespenheide, L.A. Kuhn, M.F. Thorpe, Proc. Natl Acad. Sci. 99 (2002) 3540.

[8] J.C. Phillips, Phys. Rev. Lett. (in press).

[9] R. Monasson, R. Zecchina, S. Kirkpatrick, B. Selman, L. Troyansky, Nature 400 (1999) 133.
[10] A. Feltz, H. Aust, A. Blayer, J. Non-Cryst. Solids 55 (1983) 179.
[11] R.A. Street, R.J. Nemanich, G.A.N. Connell, Phys. Rev. B18 (1978) 6915. Also see Harris J.H., Tenhover M., J. Non-Cryst. Solids 83 (1986) 272.
[12] Tanaka Keiji, Phys. Rev. B 39 (1989) 1270.
[13] C.T. Moynihan, J. Non-Cryst. Solids 172–174 (1994) 1395; 203 (1996) 359.
[14] R. Kerner, M. Micoulaut, J. Non-Cryst. Solids 176 (1994) 271.
[15] M. Micoulaut, G.G. Naumis, Europhys. Lett. 47 (1999) 568.
[16] J.H. Gibbs, E.A. DiMarzio, J. Chem. Phys. 28 (1958) 373.
[17] M.B. Meyers, E.J. Felty, Mat. Res. Bull. 2 (1967) 535.
[18] T. Wagner, S.O. Kasap, Phil. Mag. B 74 (1996) 667.
[19] D.G. Georgiev, P. Boolchand, M. Micoulaut, Phys. Rev. B 62 (2000) R9228.
[20] D.G. Georgiev, P. Boolchand, K.A. Jackson (unpublished).
[21] T. Wagner, S.O. Kasap, M. Vlcek, A. Sklenar, A. Stronski, J. Non-Cryst. Solids 227–230 (1998) 752.
[22] A. Sklenar, M. Vlcek, P. Bezdicka, in: A. Helebrant, M. Maryska, S. Kasa (Eds.), Proc. 5th ESG Conference Glass Science and Technology for the 21st Century, June 1999, Prague, Czech Republic, ISBN 80-238-3861-X, published by the Czech Glass Society, Prague, 1999, pp. C1 99.
[23] Z.U. Borisova, B.E. Kasatkin, E.I. Kim, Inorg. Mater. 9 (1973) 735.
[24] D.G. Georgiev, M. Mitkova, P. Boolchand, G. Brunklaus, H. Eckert, M. Micoulaut, Phys. Rev. B 64 (2001) 134204.
[25] L. Tichy, H. Ticha, Phil. Mag. B79 (1999) 373.
[26] L. Pauling, Nature of the Chemical Bond, Cornell University Press, Ithaca, NY, 1960, pp. 85.
[27] X.W. Feng, W.J. Bresser, P. Boolchand, Phys. Rev. Lett. 78 (1997) 4422.
[28] D. Selvanathan, W.J. Bresser, P. Boolchand, B. Goodman, Solid State Commun. 111 (1999) 619.
[29] P. Boolchand, W.J. Bresser, Phil. Mag. B 80 (2000) 1757.
[30] J.E. Griffiths, M. Malyj, G.P. Espinosa, J.P. Remeika, Phys. Rev. B 30 (1984) 6978.
[31] W.A. Kamitakahara, R.L. Cappelletti, P. Boolchand, B. Halfpap, F. Gompf, D.A. Neumann, H. Mutka, Phys. Rev. B 44 (1991) 94.
[32] P. Boolchand, R.N. Enzweiler, R.L. Cappelletti, W.A. Kamitakahara, Y. Cai, M.F. Thorpe, Solid State Ionics 39 (1990) 81.
[33] B. Effey, R.L. Cappelletti, Phys. Rev. B 59 (1999) 4119.
[34] B. Uebbing, A.J. Sievers, Phys. Rev. Lett. 76 (1996) 932.
[35] M. Frumar, Z. Polak, J. Jedelsky, Z. Cernosek, B. Frumarova, in: M.F. Thorpe, L. Tichy (Eds.), Properties and Applications of Amorphous Materials, Kluwer Academic Publishers, 2001, p. 321.
[36] W. Bues Von, M. Somer, W. Brockner, Z. Naturforsch B 35 (1980) 1063.
[37] P. Boolchand, M. Grothaus, M. Tenhover, M.A. Hazle, Grasselli, Phys. Rev. B 33 (1986) 5421.
[38] L. Cai, P. Boolchand (unpublished).
[39] Y. Wang, P. Boolchand, M. Micoulaut, Europhys. Lett. 52 (2000) 633.
[40] N. Tatsumisago, B.L. Halfpap, J.L. Green, S.M. Lindsay, C.A. Angell, Phys. Rev. Lett. 65 (1990) 1549.
[41] B.G. Aitken, C.W. Ponander, J. Non-Cryst. Solids 274 (2000) 124.
[42] C. Lyda, T. Tepe, M. Tullius, D. Lathrop, H. Eckert, J. Non-Cryst. Solids 171 (1994) 271.
[43] S. Chakravarty, D.G. Georgiev, P. Boolchand, Bull. Am. Phys. Soc. 47 (2002) 1272.
[44] Qu Tao, P. Boolchand, Bull. Am. Phys. Soc. 47 (2002) 1271.
[45] R. Mullman, B.D. Mosel, H. Eckert, Phys. Chem. Phys. 1 (1999) 2543.
[46] P. Boolchand, Insulating and Semiconducting Glasses, World Scientific Press Inc., 2000, pp. 212.
[47] S. Mahadevan, A. Giridhar, J. Non-Cryst. Solids 143 (1992) 52.
[48] Z.U. Borisova, Glassy Semiconductors, Plenum Press, New York, chapter 5, 1981.
[49] U. Tille, G.H. Frischat, K.J. Leers, in: G.H. Frischat (Ed.), Proc. 4th Int. Conf. Phys. Non-Cryst. Solids, Clausthal-Zellerfeld, 1976, pp. 631.
[50] (a) M. Micoulaut, C. R. Chimie 5 (12) (2002)
(b) P. Booslchand, D.G. Georgiev, M. Micoulaut, J. Optoelectron, Adv. Mater. 4 (2002) 823.
[51] W.J. Bresser, P. Boolchand, P. Suranyi, Phys. Rev. Lett. 56 (1986) 2493.
[52] U. Senapati, A.K. Varshneya, J. Non-Cryst. Solids 185 (1995).
[53] S. Asokan, M.Y.N. Prasad, G. Parthasarthy, E.S.R. Gopal, Phys. Rev. Lett. 62 (1989) 808.
[54] P. Boolchand, X. Feng, W.J. Bresser, J. Non-Cryst. Solids 293–295 (2001) 348.
[55] Modulated DSC Compendium (1997). Reprint #TA-210 TA Instruments Inc., New Castle, DE http://www.tainst.com/.
[56] B. Wunderlich, Y. Jin, A. Boller, Thermochim. Acta 238 (1994) 227.
[57] Y. Wang, J. Wells, D.G. Georgiev, P. Boolchand, K. Jackson, M. Micoulaut, Phys. Rev. Lett. 87 (2001) 185503.
[58] Wang Fei, P. Boolchand, K. Jackson, M. Micoulaut (unpublished).
[59] M.F. Thorpe, D.J. Jacobs, N.V. Chubynsky, A.J. Rader, in: Rigidity Theory and Applications (Ed.), M.F. Thorpe and P.M. Duxbury, Kluwer Academic Plenum Publishers, 1999, p. 239.
[60] T. Velinov, M. Gateshki, D. Arsova, E. Vateva, Phys. Rev. B 55 (1997) 11014.
[61] D. Nesheva, E. Skordeva, Phys. Status Solidi A 172 (1999) 149.
[62] P. Boolchand, J. Grothaus, J.C. Phillips, Solid State Commun. 45 (1983) 183.
[63] M. Stevens, P. Boolchand, H.J. Hernandez, Phys. Rev. B 31 (1985) 981.
[64] C.F. Niederritter, R.L. Cappelletti, P. Boolchand, Solid State Commun. 61 (1987) 527.
[65] P. Boolchand, Asian J. Phys. 9 (2000) 709.
[66] Y. Wang, K. Tanaka, T. Nakaska, K. Murase, J. Non-Cryst. Solids 299–302 (2002) 963. Also see Boukenter A., Duval E., Phil. Mag. B 77 (1998) 557.
[67] I. Petri, P.S. Salmon, H.E. Fischer, Phys. Rev. Lett. 84 (2000) 2413.
[68] C. Massobrio, R. Pasquerello, R. Car, Phys. Rev. B64 (2001) 144025.
[69] M. Cobb, D. Drabold, Phys. Rev. B56 (1997) 3054.